J. Astron. Space Sci. 14(1), 1–17 (1997)

# COLOR GRADIENTS WITHIN GLOBULAR CLUSTERS: RESTRICTED NUMERICAL SIMULATION [1]

**Young-Jong Sohn and Mun-Suk Chun**
Yonsei University Observatory, Seoul 120-749, Korea

*(Received May 5, 1997; Accepted May 20, 1997)*

## ABSTRACT

The results of a restricted numerical simulation for the color gradients within globular clusters have been presented. The standard luminosity function of M3 and Salpeter's initial mass functions were used to generate model clusters as a fundamental population. Color gradients with the sample clusters for both King and power law cusp models of surface brightness distributions are discussed in the case of using the standard luminosity function. The dependence of color gradients on several parameters for the simulations with Salpeter's initial mass functions, such as slope of initial mass functions, cluster ages, metallicities, concentration parameters of King model, and slopes of power law, are also discussed. No significant radial color gradients are shown to the sample clusters which are regenerated by a random number generation technique with various parameters in both of King and power law cusp models of surface brightness distributions. Dynamical mass segregation and stellar evolution of horizontal branch stars and blue stragglers should be included for the general case of model simulations to show the observed radial color gradients within globular clusters.

## 1. INTRODUCTION

The radial color distribution within globular clusters may occur as results of dynamical processes, which relocate stars in the system according to their masses. The integrated surface brightness distribution also reflects the present dynamical state of a globular cluster.

Bailyn (1988) attributes the color gradient in globular clusters to the spatial variation of population distribution, which is a result of mass segregation and stellar encounter or binary formation in the central region of a cluster. From the study of luminosity functions of low mass stars, Richer & Fahlman (1989) and Richer *et al.* (1991) showed the mass segregation effects within globular clusters. Recent studies for blue stragglers in globular clusters have shown that blue stragglers are more massive than red giant or subgiant stars which has similar luminosities, so that they are more concentrated to the cluster center as a result of mass segregation (Nemec & Harris 1986, Sarajedini

[1]Support for this work was provided by the Basic Science Institute Program, Ministry of Education, 1996, project No. BSRI-96-5413.

& Da Costa 1991, Sarajedini 1992, 1993). While Buonanno *et al.* (1985, 1986) and Battistini *et al.* (1985) show that redder horizontal branch stars in M15, M14, and NGC6397 are concentrated to the cluster center, Bailyn *et al.* (1986) report that blue horizontal branch stars in $\omega$ Cen are much more concentrated than the other population of stars.

Using the surface brightness profiles, Djorgovski and King (1984, 1986) classified globular clusters into the King (1966) type cluster and the post-core-collapse (PCC) cluster. PCC clusters are usually characterized by a power law cusp in the central part of their surface brightenss profiles, while traditional King type clusters have flat cores. Djorgovski (1986) shows $\sim$ 20% of Galactic globular clusters have a cusp profile. Recent studies with direct surface photometry and digital star counts suggest that color gradients do exist only in the PCC clusters in the sense of bluer center (Djorgovski *et al.* 1988, Piotto *et al.* 1988, Djorgovski *et al.* 1991a, 1991b, Djorgovski & Piotto 1993). From the color pixel histogram technique, Bailyn *et al.* (1989) and Cederbloom *et al.* (1992) also showed the existence of color gradient in the central part of the PCC cluster M15. Stetson (1991) confirmed the color gradient in M15 and suggested that the mean color of the giant and subgiant stars might be shifted blueward in the center of the cluster. On the other hand, Sohn *et al.* (1997) claim that a few clusters which have King type surface brightness profiles also show radial color gradients in the sense of bluer toward the cluster center.

In this paper, a restricted Monte-Carlo simulation with a technique of random number generation has been applied for the radial color gradient within globular clusters. For the pioneering work of color gradient by Chun and Freeman (1979), in which they reported that one third of their 24 sample clusters shows significant radial color gradient all with redder centers, Hanes & Brodie (1985), through numerical simulations, refuted that most color gradients found in Chun and Freeman's clusters can be explained by a random distribution of red giants in the innermost aperture and associated centering errors. Their simulation, however, adopted just only one standard luminosity function of M3 to regenerate the underlying population and applied to simply a family of King models. These sample models did not reflect the color distribution effects based on the different dynamical structures and different physical properties of stellar populations in a globular cluster. To complement the results of Hanes & Brodie's (1985), we adopted initial mass functions as well as a standard luminosity function to regenerate sample globular clusters. Applying the stellar evolution models to stars in the model cluster, we examine the color distribution effects with respect to metallicities, ages, and mass functions. Comparing the model clusters with a King type and a power law cusp profile, we examine the effect of dynamical states to the present color distribution in a cluster.

In Sec. 2, we discuss the fundamental stellar populations in sample clusters. The principles of regeneration of stars in sample clusters and spatial distribution of regenerated stars are presented in Sec. 3 and Sec. 4. In Sec. 5, the results of simulations are discussed. A summary of the results is given in Sec. 6.

## 2. FUNDAMENTAL POPULATIONS OF MODEL CLUSTERS

To examine the radial color and spatial population distribution within a globular cluster from the Monte-Carlo simulation based on the random number generation technique, a fundamental population distribution for a model cluster is needed. The fundamental population, which could be derived from

a photometric observation, is luminosity or mass functions. For the luminosity function, number of stars in a specific maginitude and color intervals are given. For the case of mass functions, number of stars in a specific magnitude and color interval are derived from the fitting of theoretical stellar evolution models for several masses of stars. In this paper, we have taken two different kinds of luminosity functions. One of which is provided by Hanes & Brodie (1985) for M3 as a standard luminosity function, and the other is derived from the Salpeter's initial mass functions.

**2.1 Standard Luminosity Function**

We adopted the standard luminosity function as the luminosity function of globular cluster M3, which is provided by Hanes & Brodie (1985). This sample contains 33,330 stars, and 49 bins for color and magnitude intervals. Figure 1 shows number of stars for each bins of magnitude and color, and the color magnitude diagram. Total integrated absolute magnitude and color of the sample are $M_V = -8.246$ mag and $(B-V) = 0.720$. Because the mean color of the sample is in good agreement with the photometric mean color $B-V = 0.70 \pm 0.04$ of of M3 (Peterson 1986), it seems to be reasonable to use the sample of standard luminosity function for the simulation. Moreover, magnitude interval $-2.4 \leq M_V \leq 6.01$ implicates that the sample of standard luminosty function represents the effect of color distribution from bright stars very well.

**2.2 Salpeter's Initial Mass Function**

It has been known that the initial mass functions for globular clusters are well fitted to the Salpeter's (1955) function $\xi(m) = \xi_0 m^{-(1+x)}$ through the mass range of $0.5 \leq \frac{m}{M_\odot} \leq 0.8$ (Piotto 1991, references therein). However, the slope of the mass functions ($s = 1+x$) reflect several envir-

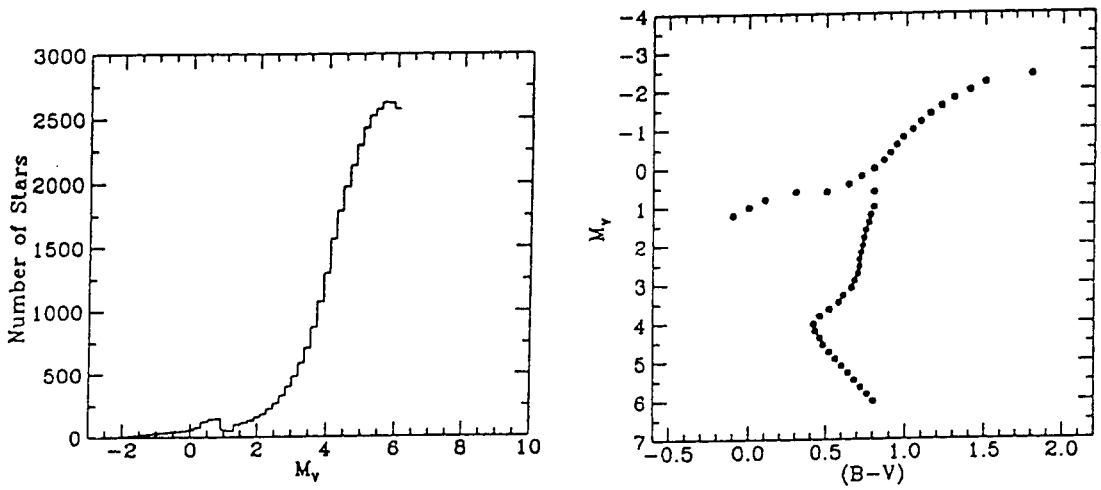


Figure 1. The standard luminosity function of M3 (left panel) and the color magnitude diagram for 49 bins of magnitudes and colors for the luminosity function (right panel).

onmental parameters of a cluster such as metallicity, position of clusters in the Galaxy, dynamical evolution of a cluster, *etc* (McClure *et al.* 1986, Pryor *et al.* 1986, Piotto 1991, Capaccioli *et al.* 1991, Richer *et al.* 1990, Lee *et al.* 1991, Drukier *et al.* 1992). Therefore, a fundamental population given by the Salpeter's initial mass functions is not likely to reflect the variation of the mass functions with respect to the dynamical evolution of a cluster. This sample, however, contains mainly the main sequnce stars and subgiant or red giant stars which have little or no mass loss effects. So, the sample derived from the initial mass functions represents the effect of color distribution from fainter stars in contrast to the standard luminosity functions very well.

## 3. THE POPULATION SCALING

To simplify the simulation, we use a present luminosity function and a present mass function not to concern about the dynamical evolution of a cluster. However, the different kinds of surface brightness distribution of clusters are well regenerated by the present luminosity or mass functions.

### 3.1 Scaling with a Standard Luminosity Function

To regenerate the number of stars in 49 bins of magnitude and color for standard luminosity function, we used a Poisson random number generator. The dispersion of mean number of stars for each bin ($N$) is given by $\sqrt{N}$. Assuming that the number of stars with the luminosity of $L_i$ is to be $\phi_i$, the dispersion of the total luminosity is given by $\sigma/L = (\Sigma_i L_i^2 \phi_i)^{1/2}/(\Sigma_i L_i \phi_i)$. With $L_V$ and $V_B$ as total luminosities of a globular cluster in $V$ and $B$ passbands, respectively, the mean error in $(B-V)$ is given by $\sigma_c^2 = (0.185)^2\, \Sigma_i \phi_i (L_{Vi}/L_V - L_{Bi}/L_B)^2$. Stars regenerated by the Poisson random number generator are distributed to the space using the uniform random number generator.

### 3.2 Scaling with a Salpeter's Initial Mass Function

Colors and magnitudes of stars in a cluster are differnt with their masses, metallicities, and cluster ages. Using the Revised Yale isochrone (Green *et al.* 1987) with different metallicities and ages, we assign the photometric properties of stars with different masses. With the minimum and maximum masses of stars ($m_L$ and $m_U$) derived from the isochrone, we generated the random numbers in accordence with the Salpeter's mass functions. In this case, we assign colors and magnitudes to $2 \times 10^5$ stars. Stars regenerated by the Salpeter's mass functions are distributed to the space using the uniform random number generator.

## 4. THE SPATIAL DISTRIBUTION OF STARS

Stars which are distributed by a uniform random number generator must be re-assigned their positions to follow the spatial density distributions of globular clusters. Two different kinds of surface density distribution functions, that is, King and power law cusp models are used as Eqs. 1 and 2,

$$f = k \left\{ \sqrt{\frac{1}{(1+(r/r_c)^2}} - \sqrt{\frac{1}{(1+(r_t/r_c)^2}} \right\}^2 \quad (1)$$

$$\log(f) = -\alpha \log(r) \quad (2)$$

where $r$ is a radius from cluster center, $f$ is a surface density, $r_c$ and $r_t$ is a core and tidal radius for a King model, and $\alpha$ is a slope for power low.

According to the dynamical structure parameters for Galactic globular clusters compiled by Trager *et al.* (1993), King type clusters have their concentration parameters ($c = log(r_t/r_c)$) in the range of 0.5 to 2.45. Djorgovski & King (1986), and Lugger *et al.* (1991) found the mean slope of power law for the PCC clusters is $\sim 0.8$.

## 5. EXAMIMATION OF THE MODELS AND DISCUSSIONS

With the standard luminosity functions, population distribution variation can be traced by the surface brightness profile property of a cluster without the information of dynamical evolution. If the Salpeter's initial mass functions were applied to the fundamental population, the effects of physical properties in globular clusters, such as metallicity, age, and mass distributions, to the radial color variation can be examined.

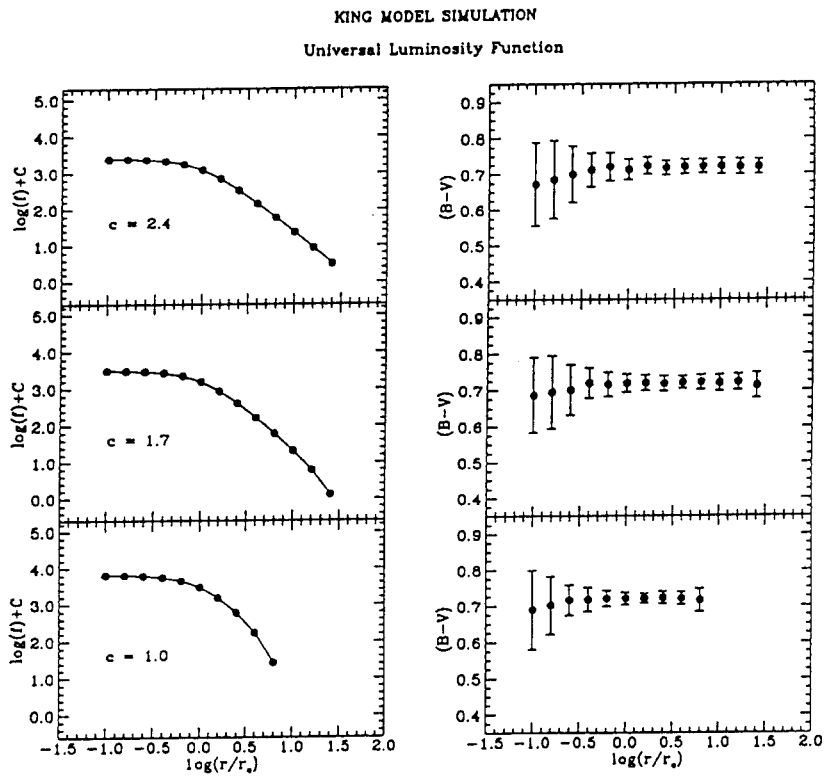


Figure 2. Surface brightness and color distribution of the King type model clusters with the standard luminosity function. $c$ represents the concentration parameter ($c = log(r_t/r_c)$) of King model.

### 5.1 Simulations with Standard Luminosity Function

With the standard luminosity function, the results are changed only with the structual parameters of globular clusters, i.e., concentration parameters $c$ for King (1966) model clusters and slopes of the power law $\alpha$ for the PCC clusters. Therefore, we have performed six different simulations for three King type cases with $c = 1.0, 1.7$, and $2.4$, and for three PCC cluster cases with $\alpha = 0.8, 1.0$, and $1.2$. Simulations were repeated 100 times for each cases and the mean values are adopted as results.

The mean magnitudes and color for the model cluster, which is regenerated from the Poisson random number generator, are calculated as $M_V = -8.248$, $M_B = -7.526$, and $(B - V) = 0.722$ with the standard errors as $\sigma_V = 0.027$, $\sigma_B = 0.021$, and $\sigma_{(B-V)} = 0.011$, respectively. Repeatability of photometric properties are in excellent agreement with the values derived from the standard luminosity function, i.e., $M_V = -8.246$, $M_B = -7.526$, and $(B - V) = 0.720$ with $\sigma_V = 0.027$, $\sigma_B = 0.020$, and $\sigma_{(B-V)} = 0.011$.

Figure 2 shows the results of King model case. In the left hand panels, we represent the King profile and concentration parameters $c$ for sample clusters. There are no distinct radial color variations for each model clusters as shown in the right panels of Figure 2. Results for the power low cusp cases are shown in Figure 3. Power law profiles and their slopes $\alpha$ are given in the left panels for each models. No distinct radial color variations are shown in the right panels.

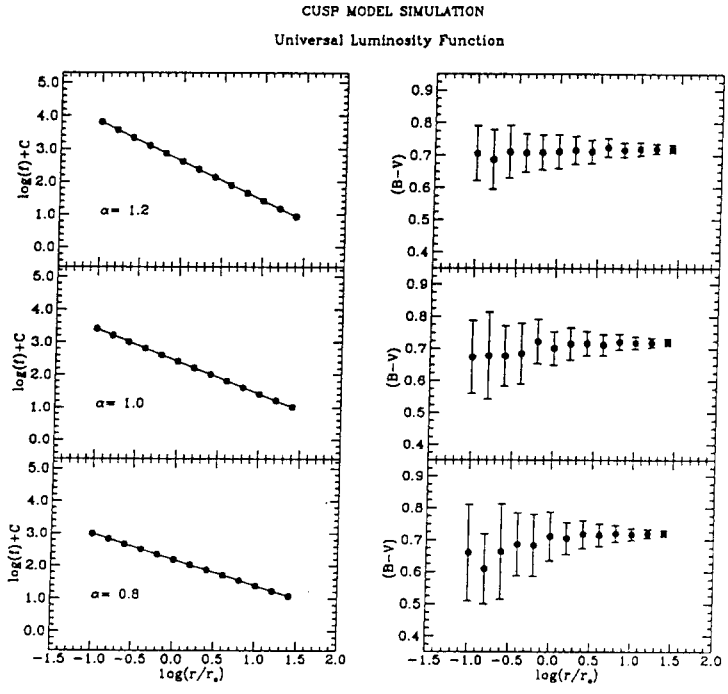


Figure 3. Surface brightness and color distribution of the power law cusp model clusters with the standard luminosity function. $\alpha$ represents the slope of power law.

Table 1. Variable parameters for simulations with Salpeter's IMFs.

| parameters | values | | |
|---|---|---|---|
| s[1] | 1.00 | 1.35 | 2.5 |
| Age[2] | 15 | 18 | 20 |
| Z[3] | 0.0001 | 0.0004 | 0.004 |
| c[4] | 1.0 | 1.7 | 2.4 |
| $\alpha$[5] | 0.8 | 1.0 | 1.2 |

Table 2. Properties of model clusters for simulations with Salpeter's IMFs.

| Fixed values | Variables | $M_V$ | $(B-V)$ | $m_U$ | $m_L$ | $M_\odot$ | $(M/L)_\odot$ |
|---|---|---|---|---|---|---|---|
| Age=20 | s = 1.00 | -8.307 | 0.707 | 0.80 | 0.52 | $1.30 \times 10^5$ | 0.73 |
| $[Fe/H] = -1.66$ | 1.35 | -8.243 | 0.706 | 0.80 | 0.52 | $1.30 \times 10^5$ | 0.77 |
| | 2.50 | -8.026 | 0.702 | 0.80 | 0.52 | $1.28 \times 10^5$ | 0.92 |
| Age=20 | $[Fe/H] = -2.26$ | -8.319 | 0.652 | 0.80 | 0.52 | $1.29 \times 10^5$ | 0.71 |
| s=1.35 | -1.66 | -8.243 | 0.706 | 0.80 | 0.52 | $1.30 \times 10^5$ | 0.77 |
| | -0.66 | -8.188 | 0.850 | 0.84 | 0.58 | $1.40 \times 10^5$ | 0.87 |
| s=1.35 | Age = 20 | -8.243 | 0.706 | 0.80 | 0.52 | $1.30 \times 10^5$ | 0.77 |
| $[Fe/H] = -1.66$ | 18 | -8.360 | 0.694 | 0.82 | 0.54 | $1.33 \times 10^5$ | 0.71 |
| | 15 | -8.376 | 0.675 | 0.86 | 0.52 | $1.35 \times 10^5$ | 0.70 |

### 5.2 Simulations with Salpeter's Initial Mass Function

To the simulations with Salpeter's initial mass functions, variable parameters are cluster ages, metallicities, slopes of the initial mass functions, and the dynamical structure parameters $c$ for King models and $\alpha$ for power law cusp models. According to the Revised Yale isochrones (Green *et al.* 1987), the age spread of globular clusters are $\sim$ 5 Gyrs with respect to the metallicity variations. Zinn (1985) found the metallicity distribution of globular clusters in our Galaxy show a bimodality with a peak of low metallicity at [Fe/H] $= -1.6$ and another pick of high metallicity at [Fe/H] $= -0.5$. Using the result from CCD photometry, Piotto (1991) found the slopes ($x = 1 - s$) of initial mass functions for 14 globular clusters are in the range between $-1.0$ and 1.7. On the other hand, Grabhorn *et al.* (1992) found that the mean $x$ value for the PCC clusters is 0.9. Durrell & Harris (1993) also found the $x$ value for the PCC cluster M15 is $0.5 \pm 0.5$.

Variable parameters used in the simulations were listed in Table 1. We fix the helium abundance $Y_{MS}$ as 0.2. Total $2 \times 10^5$ stars were used to make a sample cluster. Photometric properties, mass range of stars ($m_L$ and $m_U$, lower and upper limits of masss of stars), and mass-to-light ratios of model clusters are given in Table 2. These properties are not be affected by the different dynamical parameters of model clusters such as $c$ and $\alpha$.

To examine the color variation with respect to the variable parameters, we have performed simulations according to the following eight criteria. Each simulations repeat fifty times. The errors of colors are simple rms errors of the mean.

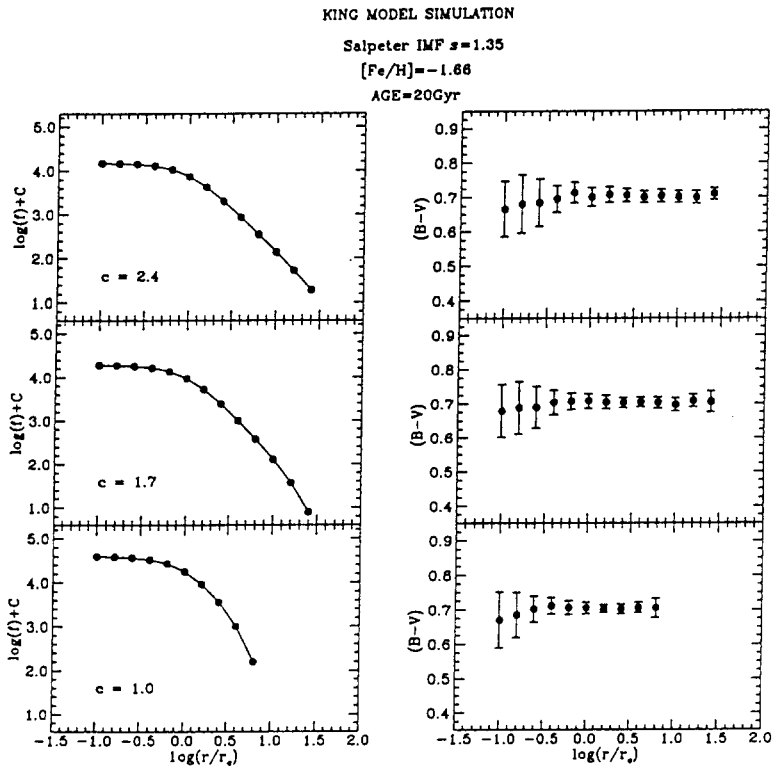


Figure 4. Surface brightness and color distribution of the King type model clusters with the initial mass functions. Constant values of age (20 Gyrs), metallicity ([Fe/H]= $-1.66$), and the slope of initial mass function ($s = 1.35$) are used to construct the model cluster. $c$ represents the concentration parameter ($c = log(r_t/r_c)$) of King model.

*Case 1)* King model surface brightness distributions with concentration parameters of $c = 1.0, 1.7,$ and 2.4, and constant values of age as 20 Gyrs, metallicity as [Fe/H]= $-1.66$, slope of initial mass function as $s = 1.35$.

Integrated magnitude and color are derived as $M_V = -8.243$ and $(B-V)= 0.706$, respectively, for every three King model cases. The results are shown in Figure 4. Solid lines in the left panels of Figure 4 represents the theoretical King profiles. Filled circles, which are the surface brightenesses derived from the simulations, are in good agreement with the theoretical values. Right panels of Figure 4 which are the $(B-V)$ color distributions of model clusters do not show any significant

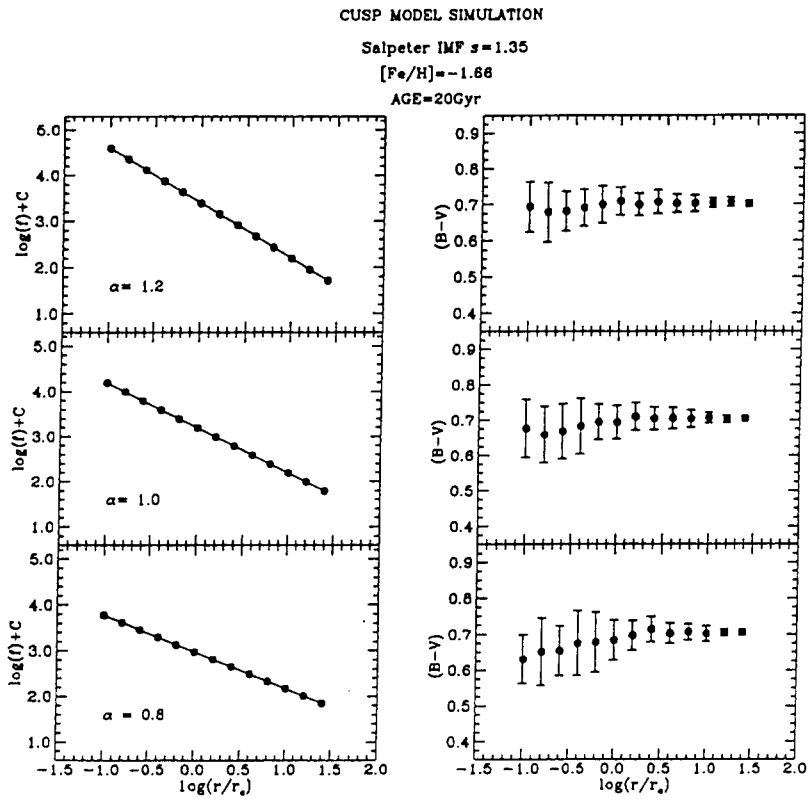


Figure 5. Surface brightness and color distribution of the power law cusp model clusters with the initial mass functions. Constant values of age (20 Gyrs), metallicity ([Fe/H]$= -1.66$), and the slope of initial mass function ($s = 1.35$) are used to construct the model cluster. $\alpha$ represents the slope of pwer law.

radial color gradient.

*Case 2)* Power law cusp model surface brightness distributions with slopes of $\alpha = 0.8, 1.0$, and 1.2, and constant values of age as 20 Gyrs, metallicity as [Fe/H]$= -1.66$, slope of initial mass function as $s = 1.35$.

Integrated magnitude and color are derived as $M_V = -8.243$ and $(B-V)= 0.706$, respectively, for every three power law cusp model cases. The results are shown in Figure 5. Solid lines in the left panels of Figure 5 represents the theoretical power law profiles. Filled circles, which are the surface brightenesses derived from the simulations, are in good agreement with the theoretical values. No

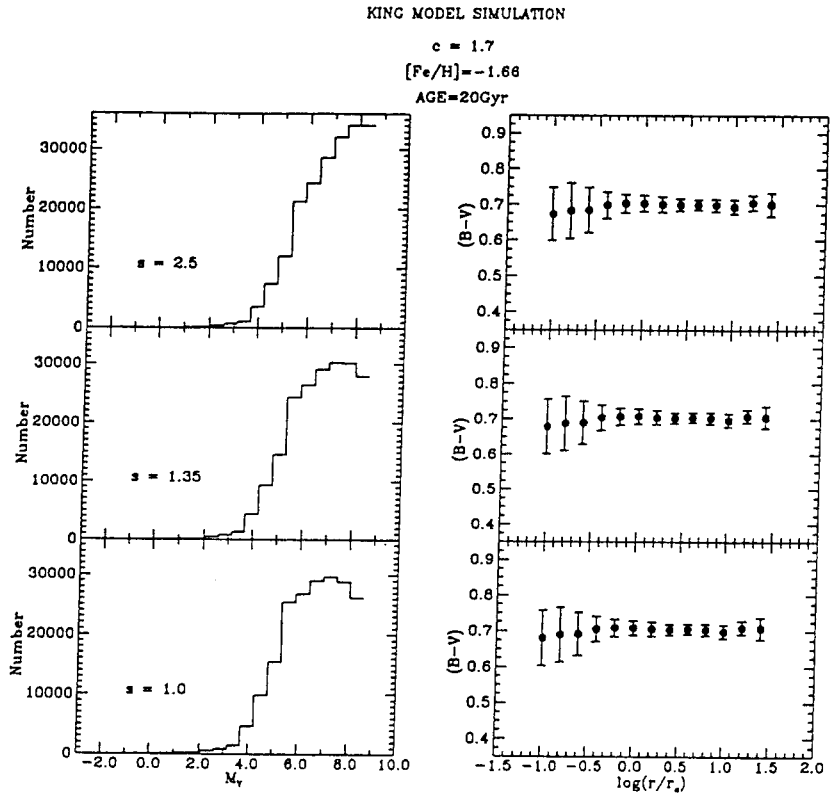


Figure 6. Luminosity functions derived from the fitting of stars in the initial mass function to isochrone and color distribution of the King type model clusters with the initial mass functions. Constant values of age (20 Gyrs), metallicity ([Fe/H]= $-1.66$), and the concentration parameter of King model ($c = 1.7$) are used to construct the model cluster. $s$ represents the slope of the initial mass function.

significant radial color gradient is shown in the right panels of Figure 5 which are the $(B - V)$ color distributions of sample clusters.

*Case 3)* Slopes of initial mass functions of $s = 1.0, 1.35$, and 2.5, and constant values of age as 20 Gyrs, metallicity as [Fe/H]= $-1.66$, concentration parameter of King model as $c = 1.7$.

Integrated magnitude and color are changed with the slopes of initial mass functions, i.e., $M_V = -8.307$ and $(B - V) = 0.707$ for $s = 1.0$, $M_V = -8.243$ and $(B - V) = 0.706$ for $s = 1.35$, $M_V = -8.026$ and $(B - V) = 0.702$ for $s = 2.5$. Stars which were regenerated by the initial mass functions are assigned magnitudes using the isochrone fitting to get the luminosity functions as

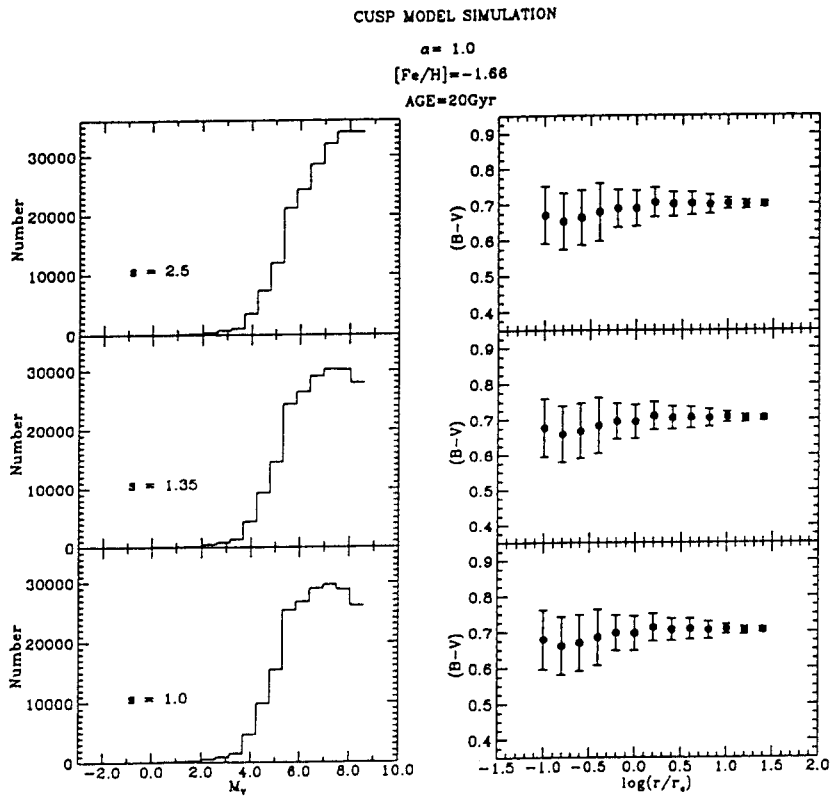


Figure 7. Luminosity functions derived from the fitting of stars in the initial mass function to isochrone and color distribution of the power law cusp model clusters with the initial mass functions. Constant values of age (20 Gyrs), metallicity ([Fe/H]= $-1.66$), and the slope of power law ($\alpha = 1.0$) are used to construct the model cluster. $s$ represents the slope of the initial mass function.

shown in the left panels of Figure 6. The larger a slope of initial mass function, the more number of faint stars. No radial $(B - V)$ color gradients are appeared with respect to the various values of slopes of initial mass function as shown in the right panels of Figure 6.

*Case 4)* Slopes of initial mass functions of $s = 1.0, 1.35$, and 2.5, and constant values of age as 20 Gyrs, metallicity as [Fe/H]= $-1.66$, slope of power law as $\alpha = 1.0$. Integrated magnitude and color are changed with the slopes of initial mass functions, and their integrated photometric properties are identical with *Case 3*. The properties of luminosity functions are also identical with *Case 3*, and shown in the left panel of Figure 7. No radial $(B - V)$ color gradients are appeared with respect to

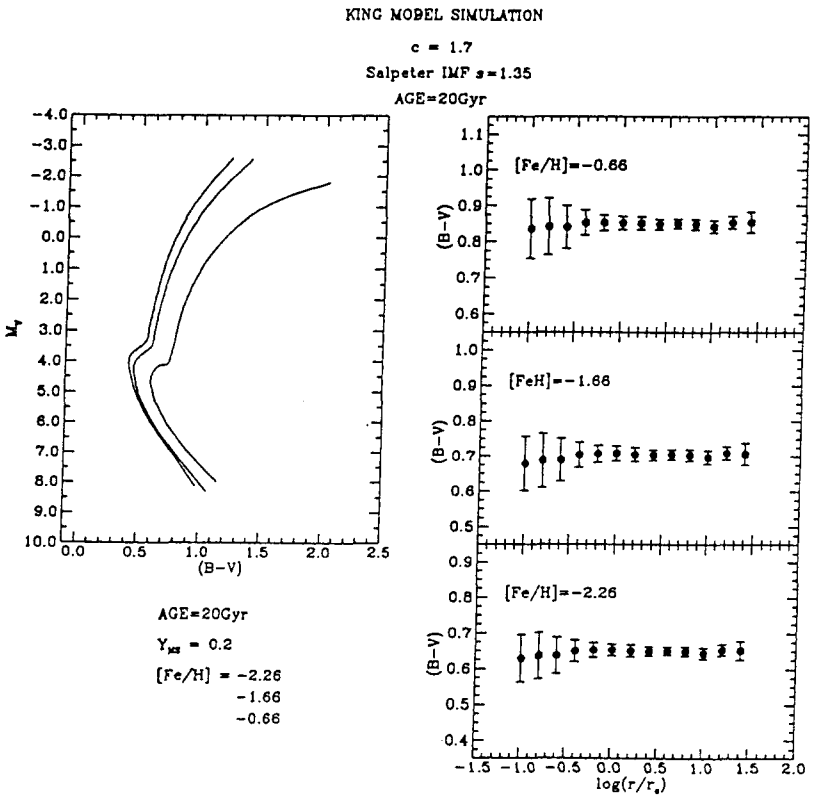


Figure 8. Isochrones with various metallicities ([Fe/H]= $-2.26, -1.66$, and $-0.66$) and color distribution of the King type model clusters with the initial mass functions. Constant values of age (20 Gyrs), the slope of initial mass function ($s = 1.35$), and the concentration parameters of King model ($c = 1.7$) are used to construct the model cluster.

the various values of slopes of initial mass functions as shown in the right panels of Figure 7.
*Case 5)* Metallicities of [Fe/H]= $-2.26, -1.66, -0.66$, and constant values of age as 20 Gyrs, slope of initial mass function of $s = 1.35$, concentration parameter of King model as $c = 1.7$. Integrated magnitude and color are changed with the metallicity [Fe/H], i.e., $M_V = -8.319$ and $(B - V) = 0.652$ for [Fe/H]= $-2.26$, $M_V = -8.243$ and $(B - V) = 0.706$ for [Fe/H]= $-1.66$, $M_V = -8.188$ and $(B - V) = 0.850$ for [Fe/H]= $-0.66$. The isochrones are shifted by changes of metallicity [Fe/H] as the left panel of Figure 8. As the metallicity is to be smaller, the isochrone

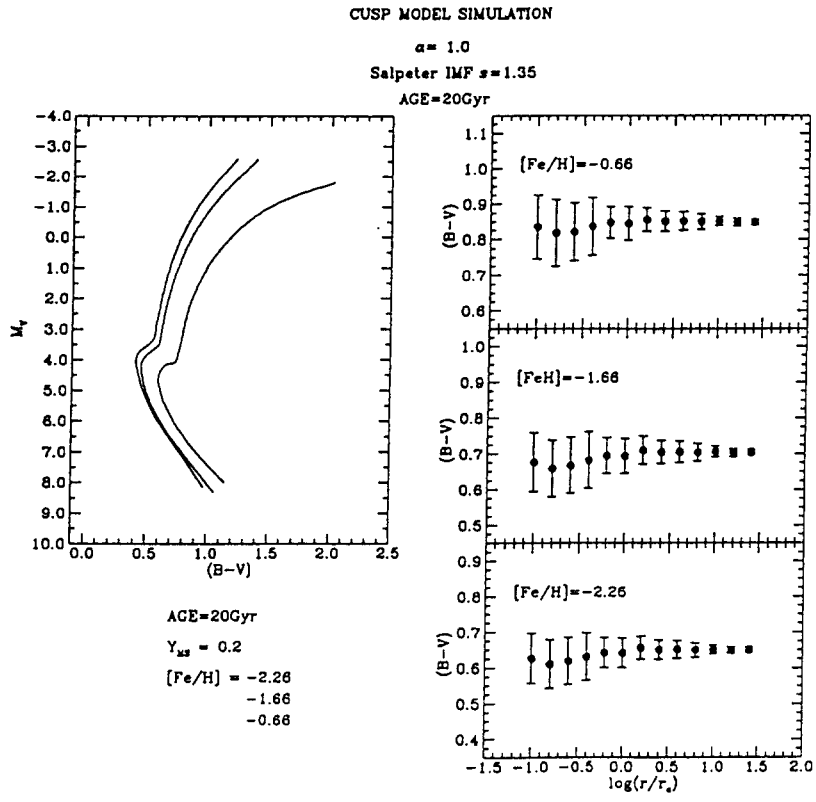


Figure 9. Isochrones with various metallicities ([Fe/H]= $-2.26, -1.66$, and $-0.66$) and color distribution of the power law cusp model clusters with the initial mass functions. Constant values of age (20 Gyrs), the slope of initial mass function ($s = 1.35$), and the slope of power law ($\alpha = 1.0$) are used to construct the model cluster.

shifts to blueward, the main-sequence turn off point are to be brighter, and the slope of red giant branch is much more steeper. Even though the integrated color of a model cluster are to be bluer with a lower metallicity, radial color gradients are not detected in the simulations.

*Case 6)* Metallicities of [Fe/H]= $-2.26, -1.66, -0.66$, and constant values of age as 20 Gyrs, slope of initial mass function of $s = 1.35$, slope of power law as $\alpha = 1.0$.

Integrated magnitude and color are changed with the metallicity [Fe/H], and their integrated photometric properties are identical with *Case 5*. The properties of isochrones are also identical with *Case 5*, and shown in the left panel of Figure 9. No radial $(B - V)$ color gradients are detected with respect to the various values of metallicities as shown in the right panels of Figure 9.

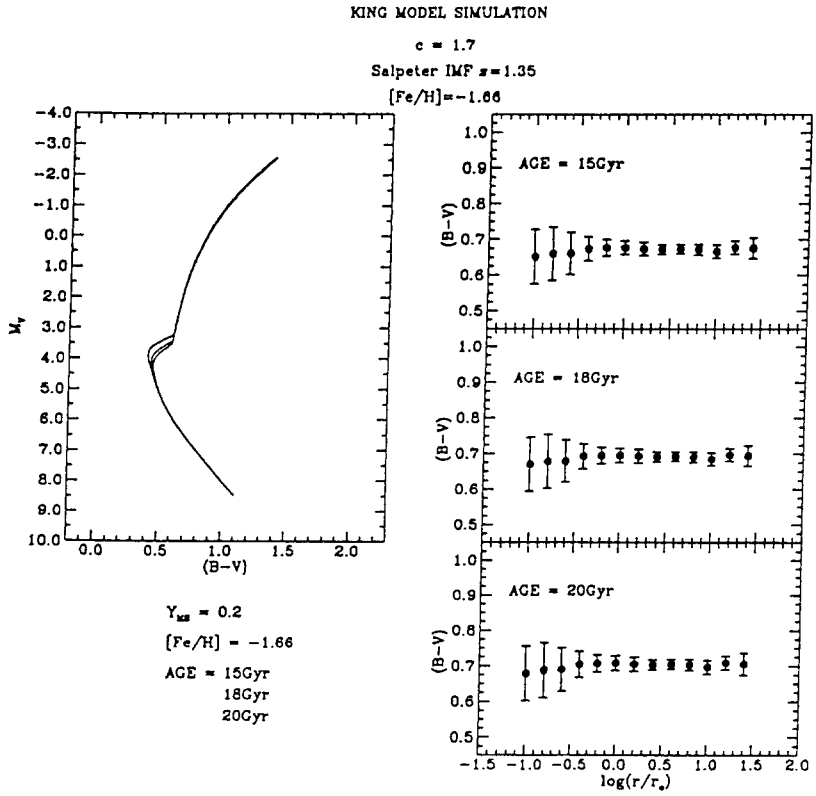


Figure 10. Isochrones with various cluster ages (15, 18, and 20 Gyrs) and color distribution of the King type model clusters with the initial mass functions. Constant values of metallicity ([Fe/H]= $-1.66$), the slope of initial mass function ($s = 1.35$), and the concentration parameters of King model ($c = 1.7$) are used to construct the model cluster.

*Case 7)* Ages of a cluster as 20, 18, and 15 Gyrs, and constant values of metallicity [Fe/H]= $-1.66$, slope of initial mass function of $s = 1.35$, concentration parameter of King model as $c = 1.7$.

Integrated magnitude and color are changed with the age, i.e., $M_V = -8.243$ and $(B-V)$= 0.706 for 20 Gyrs, $M_V = -8.360$ and $(B-V)$= 0.694 for 18 Gyrs, $M_V = -8.376$ and $(B-V)$= 0.675 for 15 Gyrs. Isochrones with ages of 15, 18, and 20 Gyrs and metallicity [Fe/H]= $-1.66$ are shown in the left panel of Figure 10. Radial color variations with respect to cluster ages are shown in the right panels of Figure 10. Although the integrated color of a model cluster is to be slightly bluer

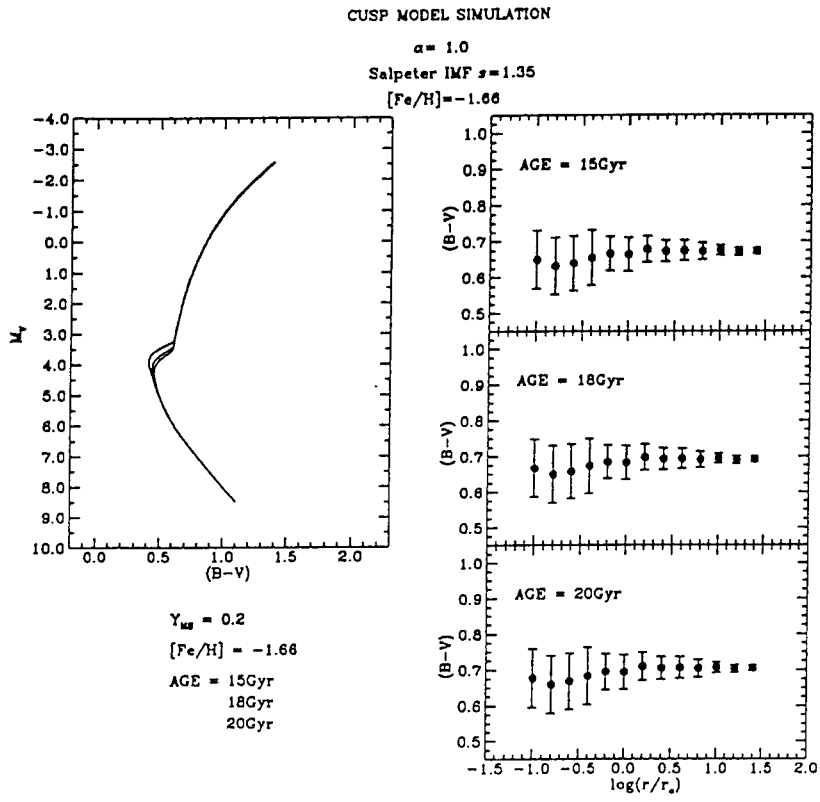


Figure 11. Isochrones with various cluster ages (15, 18, and 20 Gyrs) and color distribution of the King type model clusters with the initial mass functions. Constant values of metallicity ([Fe/H]$= -1.66$), the slope of initial mass function ($s = 1.35$), and the slope of power law ($\alpha = 1.0$) are used to construct the model cluster.

with smaller ages, no color gradients are ditected for all three cases.

*Case 8)* Ages of a cluster as 20, 18, and 15 Gyrs, and constant values of metallicity [Fe/H]$= -1.66$, slope of initial mass function of $s = 1.35$, slope of power law as $\alpha = 1.0$.

Integrated magnitude and color are changed with the age, and their photometric properties are identical with *Case 7*. The properties of isochrones are also identical with *Case 7*, and shown in the left panel of Figure 11. No radial $(B - V)$ color gradients are detected with changes of ages for model clusters as the right panels of Figure 11.

## 6. SUMMARY

The model clusters, which are generated by the random number generators using the standard luminosity function, do not show the radial color gradient for both of King and power law cusp models of surface brightness distribution. Moreover, model clusters with Salpeter's initial mass functions and photometric properties derived from the theoretical isochrones also do not show the significant radial color gradients with variable parameters such as8 slope of initial mass function, ages of clusters, metallicity [Fe/H], concentration parameters of King model $c$, and slopes of power law $\alpha$. Consequently, no color gradients has been detected on this restricted numerical simulations. However, we did not concern about the mass differences of stars in standard luminosity function and the dynamical mass segregation effects in the initial mass function models. Moreover, in the simulation with initial mass functions, horizontal branch stars and blue stragglers, which could be one of main populations to cause a color gradient, were not included in the model clusters. Therefore, dynamical mass segregation and stellar evolution of horizontal branch stars and blue stragglers must be included for the general case of model simulations.

**ACKNOWLEDGEMENTS:** YJS acknowledges the support of Korean Science and Engineering Foundation (KOSEF)'s Post-Doctoral Fellow Program.

## REFERENCES

Bailyn, C. D. 1988, in Dynamics of Dense Stellar Systems, ed. D. Merritt (Cambridge Univ. Press: Cambridge), p.167

Bailyn, C. D., Grindlay, J. E., Cohn, H. & Lugger, P. M. 1986, in IAU Symp. 126, Globular Cluster Systems in Galaxies, eds. J. E. Grindlay and A. G. D. Philip (Kluwer: Dordrecht), p.679

Bailyn, C. D., Grindlay, J. E., Cohn, H., Lugger, P. M., Stetson, P. B. & Hesser, J. E. 1989, AJ, 98, 882

Battistini, P., Bregoli, G., Fusi-Pecci, F., Lolli, M. & Epps Bingham, E. A. 1985, A&AS, 61, 487

Capaccioli, M., Ortolani, S. & Piotto, G. 1991, A&A, 244, 298

Cederbloom, S. E., Moss, M. J., Cohn, H., Lugger, P. H., Bailyn, C. D., Grindlay, J. E. & McClure, R. D. 1992, AJ, 103, 480

Buonanno, R., Corsi, C. E. & Fusi-Pecci, F. 1985, A&A, 145, 97

Buonanno, R., Corsi, C. E., Iannicola, E. & Fusi-Pecci, F. 1986, A&A, 159, 189

Chun, M.-S. & Freeman, K. C. 1979, ApJ, 227, 93

Djorgovski, S. 1986, in IAU Symp. 126, Globular Cluster Systems in Galaxies, eds. J. E. Grindlay & A. G. D. Philip (Kluwer: Dordrecht), p.333

Djorgovski, S. & King, I. R. 1984, ApJL, 277, L49

Djorgovski, S. & King, I. R. 1986, ApJL, 305, L61

Djorgovski, S. & Piotto, G. 1993, in ASPCS vol.48, The Globular Cluster Galaxy Connection, eds. G. H. Smith & J. P. Brodie (Astronomical Society of Pacific: San Fransisco), p.84

Djorgovski, S., Piotto, G. & Mallen-Ornelas, G. 1991a, in ASPCS vol.13, The Formation and Evolution of Star Clusters, ed. K. Janes (Astronomical Society of Pacific: San Fransisco), p.262

Djorgovski, S., Piotto, G., Phinney, E. S. & Chernoff, D. F. 1991b, ApJL, 372, L41
Djorgovski, S., Piotto, G. & King, I. R. 1988, in Dynamics of Dense Stellar Systems, ed. D. Merritt (Cambridge Univ. Press: Cambridge), p.147
Drukier, G. A., Fahlman, G. G. & Richer, H. B. 1992, ApJ, 386, 106
Durrell, P. R. & Harris, W. E. 1993, in ASPCS vol.48, The Globular Cluster Galaxy Connection, eds. G. H. Smith & J. P. Brodie (Astronomical Society of Pacific: San Fransisco), p.88
Grabhorn, R. P., Cohn, H. N., Lugger, P. M., & Murphy, B. W. 1992, ApJ, 392, 86
Green, E. M., Demarque, P. & King, C. R. 1987, The Revised Yale Isochrones and Luminosity Functions (Yale Univ. Observatory: New Heaven)
Hanes, D. A. & Brodie, J. P. 1985, MNRAS, 214, 491
King, I. R. 1966, AJ, 71, 276
Lee, H.-M., Fahlman, G. G. & Richer, H. B. 1991, ApJ, 366, 455
Lugger, P. M., Cohn, H. N., Grindlay, J. E., Bailyn, C. D., & Hertz, P. L. 1991, in ASPCS vol.13, The Formation and Evolution of Star Clusters, ed. K. Janes (Astronomical Society of Pacific: San Fransisco), p.414
McClure, R. D., VandenBerg, D. A., Smith, G. H., Fahlman, G. G. & Bell, R. A. 1986, ApJL, 307, L49
Nemec, J. M. & Harris, H. C. 1986, in IAU Symp. 126, Globular Cluster Systems in Galaxies, eds. J. E. Grindlay & A. G. D. Philip (Kluwer: Dordrecht), p.677
Piotto, G. 1991, in ASPCS vol.13, The Formation and Evolution of Star Clusters, ed. K. Janes (Astronomical Society of Pacific: San Fransisco), p.200
Piotto, G., King, I. R. & Djorgovski, S. 1988, AJ, 96, 1918
Peterson, C. J. 1986, PASP, 98, 192
Pryor, C., McClure, R. D., Fletcher, J. M., Hartwick, F. D. A. & Kormendy, J. 1986, AJ, 91, 546
Richer, H. B. & Fahlman, G. G. 1989, ApJ, 339, 178
Richer, H. B., Fahlman, G. G., Buonanno, R. & Fusi-Pecci, F. 1990, ApJL, 359, L11
Richer, H. B., Fahlman, G. G., Buonanno, R., Fusi-Pecci, F. Searl, L. & Thompson, I. B. 1991, ApJ, 381, 147
Salpeter, E. E. 1955, ApJ, 121, 161
Sarajedini, A. 1992, AJ, 104, 178
Sarajedini, A. 1993, in ASPCS vol.48, The Globular Cluster Galaxy Connection, eds. G. H. Smith & J. P. Brodie (Astronomical Society of Pacific: San Fransisco), p.109
Sarajedini, A. & Da Costa, G. S. 1991, AJ, 102, 628
Sohn, Y.-J., Byun, Y.-I., & Chun, M.-S. 1997, AP&SS, in print
Stetson, P. B. 1991, in Precision Photometry, ed. A. G. D. Philip (Davis: Schenectady), p.69
Trager, S. C., Djorgovski, S., & King, I. R. 1993 in ASPCS vol.50, Structure and Dynamics of Globular Clusters, eds. S. Djorgovski & G. Meylan (Astronomical Society of Pacific: San Fransisco), p.347
Zinn, R. 1985, ApJ, 293, 424